REPORT DOCUMENTATION PAGE

Form Approved
OMB No. 0704-0188

1. REPORT DATE *(DD-MM-YYYY)*	2. REPORT TYPE	3. DATES COVERED *(From - To)*
14-02-2011	Journal Article	

4. TITLE AND SUBTITLE
An Assessment of Alternative Diesel Fuels; Microbiological Contamination & Corrosion Under Storage Conditions

5a. CONTRACT NUMBER

5b. GRANT NUMBER

5c. PROGRAM ELEMENT NUMBER
0603123N

6. AUTHOR(S)
Jason Lee, Richard Ray, Brenda Little

5d. PROJECT NUMBER

5e. TASK NUMBER

5f. WORK UNIT NUMBER
73-9611-10-5

7. PERFORMING ORGANIZATION NAME(S) AND ADDRESS(ES)
Naval Research Laboratory
Oceanography Division
Stennis Space Center, MS 39529-5004

8. PERFORMING ORGANIZATION REPORT NUMBER
NRL/JA/7330-10-0331

9. SPONSORING/MONITORING AGENCY NAME(S) AND ADDRESS(ES)
Office of Naval Research
800 N. Quincy St.
Arlington, VA 22217-5660

10. SPONSOR/MONITOR'S ACRONYM(S)
ONR

11. SPONSOR/MONITOR'S REPORT NUMBER(S)

12. DISTRIBUTION/AVAILABILITY STATEMENT
Approved for public release, distribution is unlimited.

13. SUPPLEMENTARY NOTES

14. ABSTRACT
Experiments were designed to evaluate the nature and extent of microbial contamination and the potential for microbiologically influenced corrosion of alloys exposed in a conventional high sulfur diesel (L100) and alternative fuels, including 100% biodiesel (B100), ultra-low sulfur diesel (ULSD) and blends of ULSD and B100 (B5 and B20). In experiments with additions of distilled water, all fuels supported biofilm formation. Changes in the water pH did not correlate with observations related to corrosion. In all exposures, aluminum 5052 was susceptible to pitting while stainless steel 304L exhibited passive behavior. Carbon steel exhibited uniform corrosion in ULSD and L100, and passive behavior in B5, B20, and B100.

15. SUBJECT TERMS
corrosion, diesel, biodiesel, biofouling, MIC, carbon steel

16. SECURITY CLASSIFICATION OF:			17. LIMITATION OF ABSTRACT	18. NUMBER OF PAGES	19a. NAME OF RESPONSIBLE PERSON
a. REPORT	b. ABSTRACT	c. THIS PAGE			Jason Lee
Unclassified	Unclassified	Unclassified	UL	13	19b. TELEPHONE NUMBER *(Include area code)* 228-688-4494

Biofouling
Vol. 26, No. 6, August 2010, 623–635

Taylor & Francis
Taylor & Francis Group

An assessment of alternative diesel fuels: microbiological contamination and corrosion under storage conditions

Jason S. Lee*, Richard I. Ray and Brenda J. Little

Naval Research Laboratory, Codes 7332/7303, Stennis Space Center, MS, USA

(*Received 18 May 2010; final version received 26 June 2010*)

Experiments were designed to evaluate the nature and extent of microbial contamination and the potential for microbiologically influenced corrosion of alloys exposed in a conventional high sulfur diesel (L100) and alternative fuels, including 100% biodiesel (B100), ultra-low sulfur diesel (ULSD) and blends of ULSD and B100 (B5 and B20). In experiments with additions of distilled water, all fuels supported biofilm formation. Changes in the water pH did not correlate with observations related to corrosion. In all exposures, aluminum 5052 was susceptible to pitting while stainless steel 304L exhibited passive behavior. Carbon steel exhibited uniform corrosion in ULSD and L100, and passive behavior in B5, B20, and B100.

Keywords: corrosion; diesel; biodiesel; biofouling; MIC; carbon steel; aluminum; stainless steel

Introduction

Microbial contamination of hydrocarbon fuels has been recognized as a problem for over 40 years. It is the main cause of (1) clogging of fuel lines and filters, (2) product deterioration, and (3) corrosion of metals during hydrocarbon extraction, production, distribution, and storage (Videla et al. 1993). The following mechanisms for microbiologically influenced corrosion (MIC) in fuel/water systems were delineated by Videla et al. (1993): (1) a local increase in proton concentration derived from organic acidic metabolites, (2) an increase in the oxidizing characteristics of the medium, (3) metabolite production decreasing the surface energy of the passive film/electrolyte interface, (4) microbial adhesion enhancing metal dissolution, and (5) microbial uptake of fuel additives, including corrosion inhibitors. It is estimated that damage due to MIC in production, transport and storage of oil amounts to some hundred million dollars in the US every year (Costerton and Boivin 1991). Russian investigators (Agaev et al. 1986) estimated that 30% of the corrosion damage in equipment used for oil exploration and production was directly attributable to MIC.

The major limitation for microbial activity in fuels is the presence of water (Watkinson 1984). The volume of water required for microbial growth is extremely small and water is a product of the microbial mineralization of hydrocarbons. It is possible for microbial mineralization of fuel to generate a water phase for further proliferation. For example, *Cladosporium (Hormoconis) resinae* grew in 80 mg water per l of kerosene and after 4 weeks incubation, the concentration of water increased more than 10-fold (Bosecker 1996). The relationship between microorganisms, fuel and water is complicated. In general, aerobic microorganisms (fungi and aerobic bacteria) grow at the fuel water interface and anaerobic bacteria (eg sulfate-reducing bacteria) grow in oxygen-free areas (eg at the bottom of a storage tank). Nutrients are dissolved from the fuel into the water. In a freestanding clean tank most of the water is water of condensation accumulated at the bottom of the tank and amounting to a few percent of the volume of the tank. Water in fuel can also form an emulsion. Most water-in-oil emulsions are unstable and over time the water separates to the bottom of the tank. Under some circumstances bacteria and fungi can produce surfactants, causing the formation of stable water-in-oil emulsions.

The susceptibility of hydrocarbons to aerobic and anaerobic biodegradation is well known and the subject has been reviewed (Widdel and Rabus 2001; Meckenstock et al. 2004; Rabus 2005; Heider 2007; Suflita and Mclnerney 2008). It is clear that the oxidation of many different types of hydrocarbons can be coupled with the reduction of a variety of electron acceptors in addition to oxygen and that carbon dioxide is the resulting end product. It is also clear that anaerobes can couple their metabolism in syntrophic associations that ultimately allow for the

*Corresponding author. Email: jlee@nrlssc.navy.mil
Published online 12 July 2010

ISSN 0892-7014 print/ISSN 1029-2454 online

DOI: 10.1080/08927014.2010.504984
http://www.informaworld.com

conversion of the petroleum components to methane (Charkraborty and Coates 2004; Suflita et al. 2004; Townsend et al. 2004; Siddique et al. 2007; Gieg et al. 2008).

McNamara et al. (2003) demonstrated that the dominant microorganisms contaminating jet propellant (JP) fuels altered over the years with changes in formulations, refinery practices, chemical compositions, and biocides. With the introduction of ultra low-sulfur diesel (ULSD) (<15 ppm sulfur) and biodiesel, new problems may be encountered (Lockridge 2007). Londry and Suflita (1998) found that thiophenes, thiols, thiophenic acids, and aromatic sulfides, present in high sulfur diesels, could inhibit a variety of metabolic processes in anaerobic cultures enriched from an oily sludge. In addition the desulfurization processes may make low sulfur diesel more biodegradable by produeing biodegradable components (Ali et al. 2006). Biodiesels are inherently more suseeptible to microbial degradation than typical hydrocarbon fuels since methyl esters are hydrolyzed with ease under aerobic or anaerobic conditions. When mieroorganisms hydrolyze biodiesel fuels they produce fatty acids. Knothe and Steidley (2005) suggested that free fatty acids can restore lubricity to ULSD.

Experiments were designed to evaluate the nature and extent of mierobial contamination and the potential for MIC in alternative fuels, ie biodiesel, ULSD and blends of the two. L100, a conventional high sulfur diesel was included in the experiments. The main objectives of this work were: (1) to eharaeterize the corrosion and electrochemical behavior of storage and fuel tank alloys in the presence of alternative fuels over time; (2) to determine the microflora and chemistry of as-received fuels as a function of biodiesel content and storage time.

Materials and methods

Fuels

The following three neat fuels and two fuel blends were used: ULSD – 100% ULSD; L100 – 100% red dyed conventional high sulfur diesel; B100 – 100% biodiesel – soybean feedstock; B5 – 5% biodiesel/95% ULSD blend (% by volume); B20 – 20% biodiesel/80% ULSD blend (% by volume).

The first three fuels (ULSD, L100, B100) were commereially available. B5 and B20 were mixed under laboratory conditions from the ULSD and B100 supplies. One l of each of the unmixed fuels ULSD, B100, and L100 was characterized for sulfur content following ASTM D5453 (2009). Gas chromatography-mass spectrometry (GC-MS) analysis was eonducted on both pre- and post-test fuels (Johnson et al. 2004). GC-MS provided the fatty acid methyl ester (FAME) content denoted by the convention C# (number of carbons in chain).

Nine hundred ml of distilled water were added to 900 ml of fuel or fuel blend (1:1) in a 2 l crystallization dish with a watch glass cover. No further effort was made to seal the containers. Duplicate containers were prepared for each fuel. The pH of each water layer was measured post-exposure. The total exposure time was 6 months.

Microorganisms

At the onset of the experiment the natural microflora in the fuels that could be grown in distilled water was determined. For each of the neat fuels (ULSD, B100, and L100), 900 ml were combined with 900 ml sterile distilled water and placed on a shaker at 60 rpm. After 2 weeks, the water and fuel were separated using a separation funnel. Each of the water samples was sent to a commercial laboratory (Microbial Insights, Rockford, TN) for identification of microorganisms by denaturing gradient gel eleetrophoresis (DGGE) (Fischer and Lerman 1979). For baeteria, the DGGE technique separated the amplified 16S rRNA genes, whereas for fungi the 28S rRNA gene was used to form banding patterns. Banding patterns and their relative intensities were used to detect differences in mierobial communities. The most intense bands were excised and sequenced to identify mieroorganisms to the taxonomic level of genus.

To insure the presence of microorganisms in the experiments, an inoculum was used from the sludge layer in a tank containing L100. The inoculum was prepared by combining 300 ml of the sludge with 2 l of sterile distilled water and placed on a shaker at 60 rpm. After 2 weeks, the water layer was separated from the sludge using a separation funnel. The sludge was discarded. The microflora present in the water layer was eharaeterized using the teehniques previously described. Twenty ml of the water layer inoculum were added to each experimental container at the start of the experiment. No attempt was made to sterilize the glassware, eoupons, wires, or plastie mounts prior to introduction of fuel/water eombinations. At the eonclusion of the 6-month exposure, mieroorganisms in water layers from the 10 containers were identified as previously described.

Metals

Carbon steel UNS C10200 (C1020), stainless steel UNS S30403 (SS304L), and aluminum alloy UNS A95052 (AA5052) were selected as representative fuel tank alloys (Table 1). Metal eoupons of eaeh alloy were obtained from Metal Samples, Inc. (Munford,

Table 1. Chemical compositions of alloys in wt% (Davis 1998).

Alloy	C	Mn	P	S	Si	Cr	Ni	N	Al	Cu	Fe	Mg	Zn
C1020	0.20	0.47	0.012	0.013							Bal.		
304L	0.021	1.35	0.031	0.004	0.41	18.11	8.39	0.15		0.141	Bal.		
5052		0.1			0.15	0.15–0.35			Bal.	0.10	0.40	2.26	0.1

AL, USA) with dimensions of 1.6 cm diameter and 0.32 mm thick. An insulated wire was attached to the backside of each coupon with conductive epoxy and carbon tape to achieve electrical connection. Coupons were individually mounted in Epothin epoxy (Buehler Ltd, Lake Bluff, IL, USA) to electrically isolate the wire connection and to establish an exposed area of 2 cm^2. Each coupon was wet-polished to a 600-grit finish, sonicated in soapy water, rinsed with acetone, and dried with nitrogen gas.

Three epoxy-mounted coupons of each alloy were used in each of the five fuel/water combinations. Coupons were vertically orientated in the exposure vessels at the fuel/water interfaces. AA5052 and SS304L coupons were exposed in the same container, while C1020 coupons were exposed separately. A mercury/mercury sulfate ($Hg/HgSO_4$) electrode and a 4 cm^2 platinum-niobium mesh were used as reference and counter electrodes, respectively, in a standard three-electrode electrochemical setup. The sulfate-based reference electrode was chosen over a chloride containing reference electrode (eg saturated calomel, silver/silver-chloride) to avoid possible chloride contamination. A Luggin probe filled with saturated potassium sulfate solution was used to decrease the effect of voltage drop. The Luggin probe was removed after measurements to minimize sulfate contamination.

A computer-controlled potentiostat (Gamry Instruments, Warminster, PA, USA) was used for all electrochemical measurements. For each measurement, the Luggin probe was positioned at the fuel/water interface to within 5 mm of the coupon surface. Solution resistance (R_s) between the coupon and the Luggin probe was determined by electrochemical impedance spectroscopy (EIS). The measured impedance at the highest frequency with a phase angle > -5 degrees was recorded as R_s. All distilled water/fuel combinations had significant R_s values within the range of 10^4 to 10^7 ohms. The corrosion potential (E_{corr}) was recorded for each coupon *vs* the reference electrode. The polarization resistance (R_p) was determined using the linear polarization resistance (LPR) technique as detailed in ASTM Standard G59 (2003a). Current was recorded as the potential of each coupon was scanned from -10 mV to $+10$ mV *vs* E_{corr}. A slow scan rate of 0.16 mV s^{-1} was used during LPR to compensate for the lack of charge carriers in solution. R_p was determined from the Ohm's Law relationship:

$$V = I \times (R_p + R_s) \quad (1)$$

where V is potential and I is current. Solving for R_p results in,

$$R_p = \frac{V}{I} - R_s \quad (2)$$

where the slope of the LPR measurement (V/I) (determined by least squares fit) less the EIS measured R_s gives R_p. A commercial program, Echem Analyst v5.5 (Gamry Instruments, Warminster, PA, USA), was used to automate R_p determination. The inverse (R_p^{-1}) is proportional to the instantaneous corrosion rate. The term 'instantaneous' is used to differentiate the rates from cumulative corrosion rates. R_p, R_s, and E_{corr} ($V_{Hg/HgSO4}$) were measured every 1 to 2 weeks for all exposed samples and averaged for each triplicate set of alloy/fuel combinations. R_p^{-1} trends were normalized for electrode area (2 cm^2) and are reported in units of ohms^{-1} cm^{-2}. Laboratory temperature was maintained at 23°C with fluorescent lighting for 8 h a day.

After 6 months, each coupon was removed, fixed in 4% glutaraldehyde buffered with 0.1 M sodium cacodylate (pH 7.2) and stored in a refrigerator at 4°C. Fixed coupons were imaged using a digital camera and rinsed through a graded series of distilled water/acetone to remove fuel and water. Coupons were further rinsed through a graded series of acetone/xylene to remove acetone and residual fuel and allowed to air dry (Ray and Little 2003). Coupons were imaged in an environmental scanning electron microscope (ESEM) at an accelerating voltage of 20 kev and a chamber water vapor pressure of 2–4 torr.

Select coupons were removed from the epoxy mount and acid cleaned to remove corrosion products. C1020 coupons were acid cleaned according to ASTM G1 (2003b) for 10 min in a room temperature solution of 500 ml concentrated hydrochloric acid (SG 1.19), 3.5 g hexamethylene tetramine and deionized water to make 1 l. AA5052 coupons were acid cleaned in concentrated nitric acid (SG 1.42) for 1 min at room temperature. It was not necessary to clean SS304L

coupons. Coupons were scanned using a Nanovea (Irvine, CA) Model PS50 non-contact optical profiler with a 3.5 mm optical pen to reconstruct high contrast 3-D digital images. Pit depths were measured from these reconstructions. Pitted coupons were re-embedded in epoxy and cross-sectioned on a slow speed diamond saw. Cross-sections were examined with an ESEM and a dissecting microscope with attached digital camera.

Results

Fuels

Pre-exposure B100 fuel was composed of C17 and C19 FAME as determined by GC-MS. After 6 months C21, C23, and C25 FAME were also detected. All L100 fuels had a 10% FAME (C17 + C19) content indicating a conventional diesel/biodiesel blend. All ULSD fuels (pre- and post-exposure) had a 0% FAME content indicating no biodiesel blending. The sulfur concentration in L100 was 1273 ppm; in B100, 3 ppm; and in ULSD, 2 ppm. A color change was observed in all biodiesel exposures (Figure 1). The initial dark yellow color was masked by a bright green color after 3 months in B100, 4 months in B20 and 4.5 months in B5. Over the same 6-month period, B100 stored in an opaque sealed container with no added water, metal samples or inoculum, retained the original yellow color.

The pH of distilled water used in the experiments was 5.75. After the 6-month exposure to the different fuels, the pH of the water layers was measured (Table 2). The highest pH, 6.64, was measured for ULSD exposed to C1020. The lowest pH, 3.41, was measured for L100 exposed to C1020. The pH values measured in fuels containing biodiesel had intermediate values. Increasing biodiesel content corresponded with lower pH values.

After 6 months containers with ULSD and C1020 contained dark orange precipitates at the bottom of the water layer, presumably iron corrosion products. All containers showed evidence of biofouling at the fuel/water interface and in the water layer.

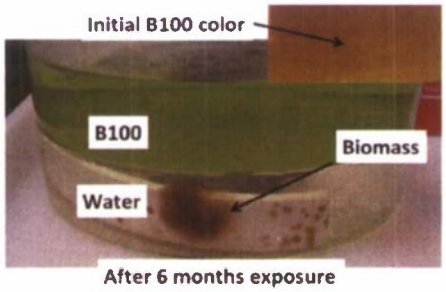

Figure 1. Biomass in the water layer after 6 months in B100. In addition, the color change to the bright green can be seen. Insert shows the original B100 color.

Microorganisms

The inoculum contained *Niastella*, *Acinetobacter*, *Bacillus*, *Rhodotorula*, and *Mycosphaerella*. Predominant microorganisms in water exposed to fuels after 2 weeks and 6 months are listed in Table 3. After 2 weeks all samples contained both bacteria and fungi except L100, where no fungi were identified. After 6 months, *Sphingomonas* was identified in ULSD, B5 and B20. *Aureobasidium* and *Paecilomyces* were identified from biodiesel-containing fuels. *Rhodotorula*, found in B20, was the only microorganism originating from the inoculum that could be identified in a post-exposure fuel after 6 months. For each fuel/water combination, species diversity generally decreased over the 6 months.

Metals

SS304L

There were no visual indications of corrosion in SS304L after 6 months in any fuel/water combination. E_{corr} values ranged from 0.15 to -0.3 $V_{Hg/HgSO4}$ with L100 and ULSD having the highest and lowest values, respectively. SS304L exposed in biodiesel-containing fuels exhibited the lowest R_p^{-1} (10^{-7} ohm^{-1} cm^{-2}). However, R_p^{-1}in B100 increased to 10^{-6} ohm^{-1} cm^{-2} after 6 months. A distinct biofilm of bacteria and fungi was associated with the fuel/water interface and in the water phase. Above the interface, fungi and bacteria were sparsely attached to the metal surface.

C1020

E_{corr} and R_p^{-1} trends (triplicate averaged) for C1020 exposed in each of the 5 fuel/water combinations are shown in Figure 2a and b, respectively. Exposure to ULSD produced the highest R_p^{-1} (10^{-3} ohm^{-1} cm^{-2}) (2 orders-of-magnitude higher than L100) and the

Table 2. pH values of water layers after 6-months exposure to fuel and alloys.

Fuel	C1020	SS304L + AA5052
ULSD	6.64	4.98
L100	3.41	3.49
B5	5.80	4.93
B20	4.64	5.21
B100	3.97	3.85

Initial distilled water pH = 5.75.

Table 3. Bacterial and fungal populations of water layers after 2-weeks and 6-months exposures to fuels.

Fuel	Bacteria		Fungi	
	2 weeks	6 months	2 weeks	6 months
ULSD	*Bradyrhizobium, Chelatococcus, Sphingomonas,*	*Sphingomonas*[a]	*Paecilomyces*	*Aureobasidium*[a]
B5	*Bradyrhizobium, Chelatococcus, Methylobacterium, Sphingomonas*	Alphaproteobacteria[a,b], Betaproteobacteria[b], *Sphingomonas*[a,b]	*Aureobasidium, Cryptococcus, Paecilomyces*	*Calosphaeria*[a], *Paecilomyces*[b]
B20	*Bradyrhizobium, Chelatococcus, Methylobacterium, Sphingomonas*	Alphaproteobacteria[a,b], *Sphingomonas*[b]	*Aureobasidium, Cryptococcus, Paecilomyces*	*Rhodotorula*[a,c]
B100	*Methylobacterium, Sphingomonas*		*Aureobasidium Cryptococcus*	*Aureobasidium*[a] *Paecilomyces*[b]
L100	*Bacillus, Thermomonas*			*Hormoconis*[a], *Saccharomyces*[a]

[a]C1020; [b]SS304L + AA5052; [c]from inoculum.

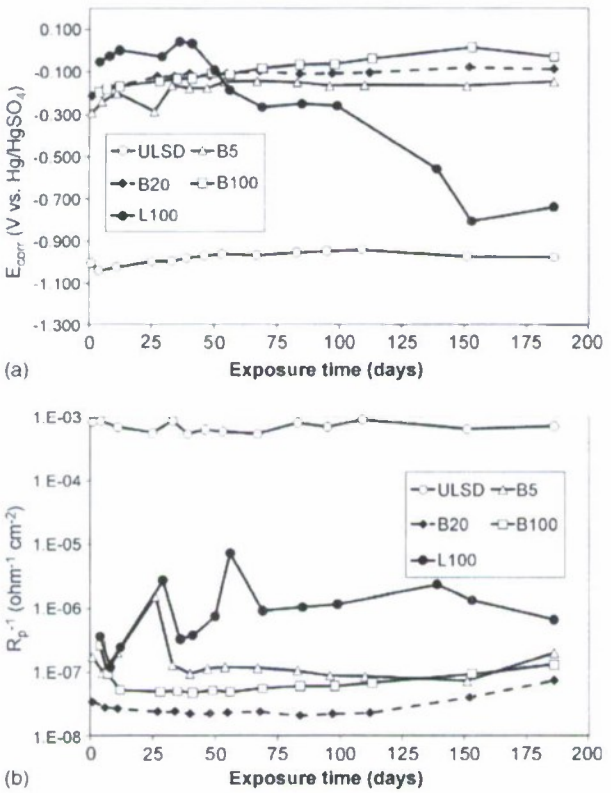

Figure 2. (a) E_{corr} ($V_{Hg/HgSO4}$) and (b) R_p^{-1} (ohm^{-1} cm^{-2}) trends for C1020 exposed in each of the 5 fuel/water combinations.

lowest E_{corr} values (-1.0 $V_{Hg/HgSO4}$). C1020 in L100 had the second highest R_p^{-1} with intermittent spikes of an order-of-magnitude increase at days 29 and 56. E_{corr} started out at ~ 0.0 $V_{Hg/HgSO4}$ but by day 150, had dropped to -0.8 $V_{Hg/HgSO4}$. In general, biodiesel-containing fuels had similar low R_p^{-1} (10^{-7} ohm^{-1} cm^{-2}) and stable E_{corr} values ranging from 0.0 to -0.3 $V_{Hg/HgSO4}$ over the entire 6-month exposure.

After 4 days, orange corrosion products were obvious on all C1020 exposed in ULSD and distilled water below the fuel/water interface. In comparison, C1020 exposed in B100 only had discoloration at the fuel/water interface. After 6 months, C1020 exposed in ULSD resulted in large amounts of dark orange corrosion products at and below the fuel/water interface (Figure 3a). General corrosion without pitting occurred below the interface (Figure 3b and c). C1020 exposed in B5 (or B20) did not result in corrosion and polishing marks were still visible on the surface (Figure 4a). Biofilms, containing both bacteria and fungi, developed above, at and below the fuel/water interface. Fungal hyphae with spores (Figure 4b) and rod-shaped bacteria were attached to C1020 on and below the interface. C1020 exposed in L100 resulted in a thick dark red deposit at the fuel/water interface (Figure 5a). Acid cleaning revealed a distinct band of corrosion at the interface with minimal attack in the fuel layer (Figure 5b and c). Below the interface, pitting (200 μm deep) and uniform etching were observed. All C1020 results were replicated in triplicate exposures.

AA5052

E_{corr} and R_p^{-1} trends for AA5052 exposed in each of the 5 fuel/water combinations are shown in Figure 6a and b, respectively. E_{corr} values ranged from -0.5 to -1.25 $V_{Hg/HgSO4}$. E_{corr} for the L100 exposure dipped to -1.25 $V_{Hg/HgSO4}$ in the first 7 days in comparison to the B100 exposure that increased to -0.7 $V_{Hg/HgSO4}$. After 30 days, the L100 exposure had increased to -0.7 $V_{Hg/HgSO4}$, the same level as B100. B5, B20, and ULSD exposures all exhibited E_{corr} trends that increased by ~ 0.2 V over the 6-month period. In

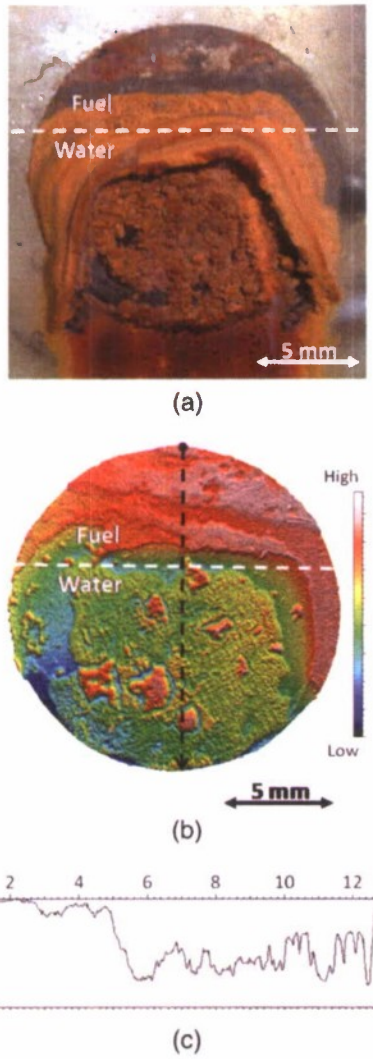

Figure 3. (a) C1020 after 6-months exposure in ULSD and distilled water with visible corrosion at and below the fuel/water interface. (b) Acid cleaned surface reconstructed by 3-D profilometry. (c) Cross-sectional profile shows the majority of metal loss occurred at and below the fuel/water interface (black dashed arrow in b).

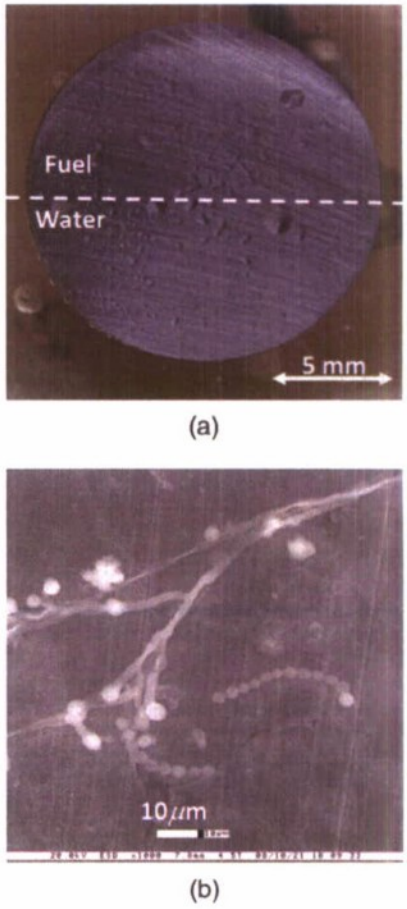

Figure 4. (a) C1020 after 6-months exposure in B5 and distilled water exhibited no evidence of corrosion as indicated by the intact polishing marks on the surface. (b) Fungal hyphae and spores attached to a C1020 surface at the fuel/water interface.

contrast, after the initial increase, L100 and B100 E_{corr} trends decreased by ~0.1 V over the 6-month exposure period. E_{corr} trends coincided with increased R_p^{-1} for L100 and B100 over time and decreased R_p^{-1} for B5, B20, and ULSD exposures. R_p^{-1} in L100 increased from 10^{-6} ohm^{-1} cm^{-2} to 10^{-4} ohm^{-1} cm^{-2} over the 6-month. The next highest R_p^{-1}, measured in the B100 exposure, was 2 orders-of-magnitude lower.

A build-up of corrosion products and biofilm was observed on all AA5052 coupons at the fuel/water interface. All AA5052 surfaces were pitted in the fuel phase, at the interface and in the water phase. The deepest pits were measured in L100 and distilled water (Figure 7a–e). Pits above the interface were as large as 700 μm in diameter with maximum penetration of 650 μm (Figure 7b and e). A cross-section of two adjacent pits at the interface demonstrated that the two pits were joined below the surface (Figure 7d). A shallow pit (200 μm diameter, 100 μm deep) formed above the interface was cross-sectioned (Figure 7e). The cross-section exposed extensive corrosion beneath the surface with crack-like morphology. Over the entire surface of the coupons, small pits (<1 μm diameter) within larger pits were observed. In the case of ULSD a pit above the interface was 350 μm in diameter and 600 μm deep, whereas the pit at the interface had the same penetration depth but was over 1 mm in diameter.

After the 6-month exposure to B5, B20, and B100 and distilled water all AA5052 surfaces were pitted in

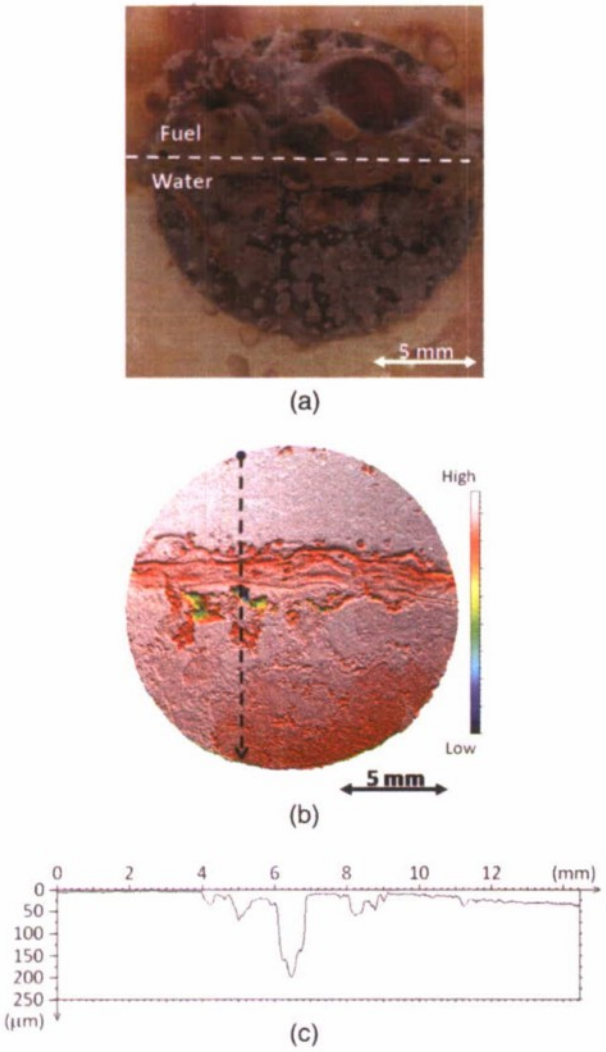

Figure 5. (a) C1020 after 6-months exposure in L100 and distilled water with build-up at fuel/water interface. Profilometry of acid cleaned surface (b) and cross sectional profile (c) (black dashed line) revealed minimal attack in the fuel layer, and a distinct band of corrosion at the interface with associated pits and light etching in the water layer.

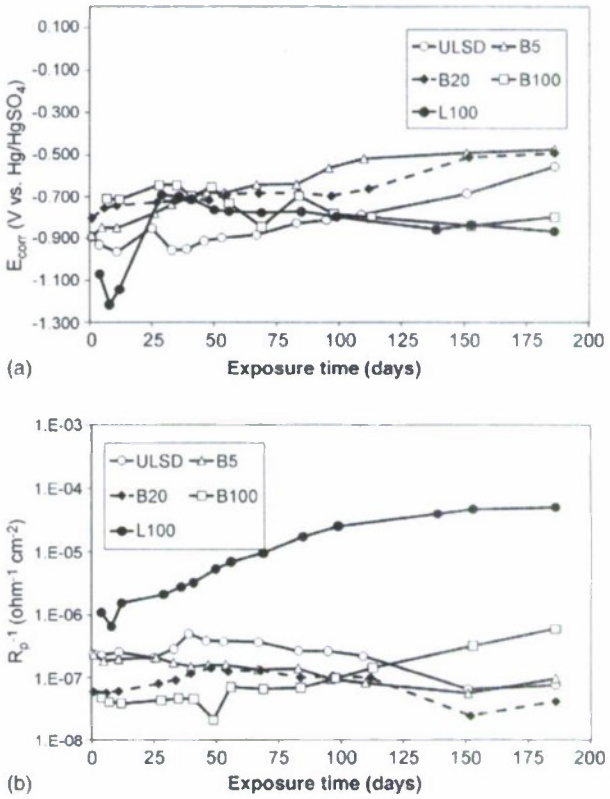

Figure 6. (a) E_{corr} ($V_{Hg/HgSO4}$) and (b) R_p^{-1} (ohm^{-1} cm^{-2}) trends for AA5052 exposed in each of the 5 fuel/water combinations.

the fuel phase, at the interface and in the water phase. In the case of B5 a 275 μm diameter hemispherical pit was located above the interface. Fungal hyphae and spores were located at the interface. Below the interface in the water layer, small 1–5 μm diameter pits were found. In the case of B100, pits above the interface were as large as 1.5 mm in diameter with maximum penetration of 650 μm. Pits at the interface measured (by profilometry) 100 μm in diameter and 200 μm deep with crystallographic corrosion morphology (Figure 8). Most of the metal loss occurred below the metal surface with a pit depths >500 μm and could only be detected in cross-section (Figure 9). The spatial distribution of corrosion was consistent with distance from the fuel/water interface among replicates.

Discussion

Experiments described in this paper were designed to characterize the corrosion of storage tank alloys exposed to alternative fuels and to relate that corrosion to the microflora that developed in the presence of distilled water. It was the intention to use a conventional fuel (L100) for comparison purposes. However, the presence of C17 and C19 FAME in commercially available L100 demonstrates the complexity of the present commercial fuel situation. The FAME was not due to experimental effects, but was most likely the result of evitable mixing that has and will continue as alternative fuels are introduced into previously used tanks. The presence of C21, C23 and C25 FAME and the color change observed in all exposures containing biodiesel

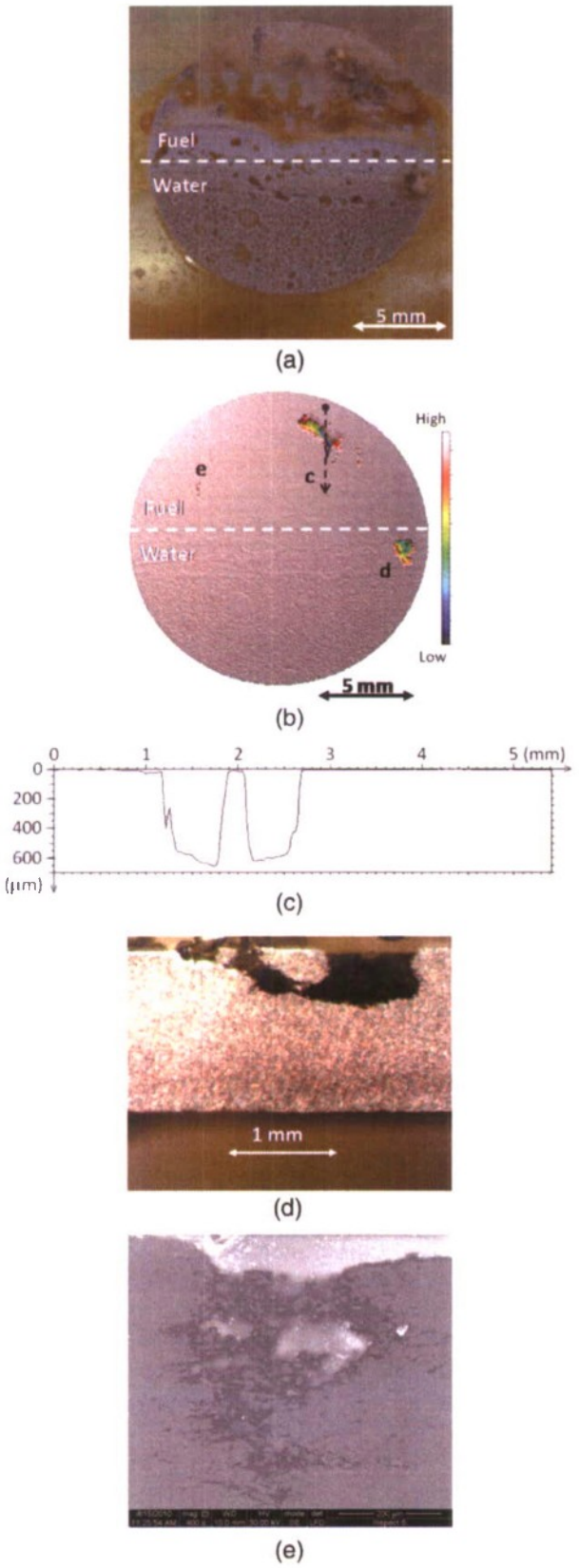

was most likely the result of photosynthetic algal growth.

It is difficult to compare studies on biofouling and corrosion in the presence of alternative fuels because experiments have been conducted under varying conditions with varying fuels. Most investigators have reported that there is little or no corrosion of metals exposed to neat low- or no-sulfur biodiesels over short exposures. Using weight loss and R_p^{-1} as indicators of corrosion, Meenakshi et al. (2010) concluded that the corrosion rates of aluminum, carbon steel, copper, and brass exposed in neat biodiesel (B100) (derived from *Pongamia pinnata*) for 100 h were insignificant. Addition of 1% NaCl did not increase the corrosion rate. In other studies (Kaul et al. 2007), biodiesel from the *Salvadora* plant produced corrosion on metal parts of a diesel engine whereas biodiesel from other oils caused little or no corrosion. Corrosion in the presence of the *Salvadora* biodiesel was attributed to high sulfur compounds (sulfur 1600 ppm).

Biodiesels are hygroscopic and typically contain approximately 1200 ppm water absorbed from the atmosphere. In the presence of water, biodiesels support the growth of aerobic and anaerobic microorganisms. The rate of degradation of soybean methyl biodiesel is reportedly as fast and complete as that of glucose by the action of soil microbial populations (Zhang et al. 1998). Lutz et al. (2006) reported that palm methyl or ethyl biodiesel was degraded aerobically by wild-type bacteria. Aktas et al. (2010) observed that soy-based biodiesel was hydrolyzed and converted to a variety of fatty acid intermediates by anaerobic microorganisms, regardless of previous hydrocarbon- or biodiesel-exposure history.

DGGE of PCR-amplified 16s RNA gene fragments is a common technique for examining natural bacterial communities (Jackson et al. 2000). Muzer and Smalla (1998) reviewed the applicability of the technique in microbial ecology and Wang et al. (2008) used the technique to monitor bacteria during microbial enhanced oil recovery. In the present study, microorganisms were identified in the distilled water that had been in contact with fuels. Since it is unlikely that alternative fuels will be added to pristine tanks, the inoculum was prepared from sludge in a tank that had contained conventional diesel. However, the microorganisms from the inoculum did not grow over the 6-month

Figure 7. (a) AA5052 after 6-months exposure in L100 and distilled water. (b) Acid cleaned surface reconstructed by 3-D profilometry. (c) Cross-sectional profile of deep (650 μm) pits in the fuel layer (black dashed arrow in (b). (d) Cross-section of two adjacent pits at the fuel/water interface joined below the surface. (e) Cross-section of pit with crack-like morphology.

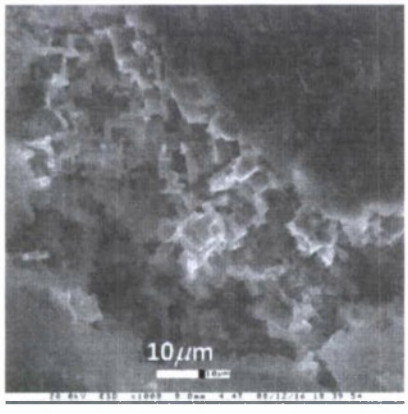

Figure 8. Pit in AA5052 after 6-months exposure in B100 and distilled water with crystallographic morphology.

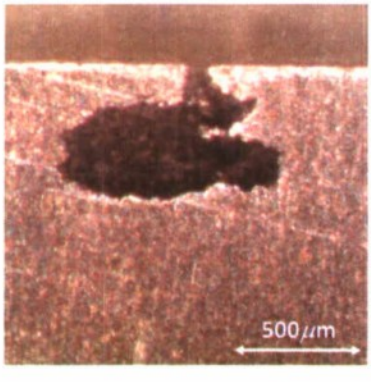

Figure 9. Pit cross-section in AA5052 after acid cleaning.

exposure and only one of the organisms in the original inoculum, *Rhodotorula*, was identified in one of the water samples after 6-month exposures. There were no consistent patterns for predicting the organisms in the water after 6 months based on the organisms detected in the original fuel, fuel blend, or the inoculum. *Sphingomonas* was the most prevalent organism among the samples (Table 3). *Cladosporium* (*Hormoconis*), the organism most closely related to corrosion in hydrocarbon fuels (Churchill 1963; Hendey 1964; Videla et al. 1993) was detected in L100 at the conclusion of the experiment. While it was not possible to identify the microorganisms that survived the experimental conditions using DGGE, all of the fuels and fuel blends used in these studies supported the development of a biofilm containing bacteria and fungi, particularly at the fuel/water interface, when exposed to distilled water. There are several limitations to the DGGE technique. Individual bands may not be due to a single unique DNA sequence, ie two sequences differing by more than one base pair could co-migrate to identical positions in DGGE gels (Jackson et al. 2000). The result would be an underestimation of population diversity. Furthermore, an organism must constitute approximately 2% of the total population to be detected by DGGE.

In the present experiments the pH of the water layer changed after exposure to fuels, metals and microorganisms. As shown in Table 2, an increased biodiesel content resulted in a decreased bulk water pH. This trend has been demonstrated previously by Grainawi (2009). L100 contained 10% biodiesel that may have been partially responsible for the decreased bulk water pH. Production of microbial metabolites, such as acids, and hydrolysis of metal cations may have contributed to pH changes. Melero et al. (2010) suggested that increased acidity in vegetable oils and animal fats might cause increased corrosion.

The metals used in the present studies (C1020, SS304L, and AA5052) are routinely exposed to fuels either in storage or in fuel transfer lines. All the metals have been investigated and mechanisms for localized corrosion, including MIC, have been documented. In most cases localized corrosion and MIC of SS304L is attributed to under deposit corrosion in a chloride-containing fresh water medium. In the case of MIC the deposit is caused by bacteria, particularly iron-depositing bacteria. Despite the presence of a biofilm at the fuel/water interface in the present studies, there were no visible or electrochemical indications of localized corrosion of SS304L.

Biofilms were identified on C1020 in all fuel/water combinations and most readily observed at the fuel/water interface. Biofilms of bacteria and fungi were associated with regions of active corrosion (ULSD, L100) and with intact surfaces (B5, B20, B100). Reddish-orange corrosion products were visible on C1020 after 4 days exposure in ULSD with distilled water. After 6 months, voluminous corrosion products at the fuel/water interface were observed after exposure to ULSD and L100. The lowest E_{corr} (-1.0 $V_{Hg/HgSO4}$) and highest R_p^{-1} (10^{-3} ohm^{-1} cm^{-2}) were also measured in the C1020 exposure to ULSD (Figure 2a and b). Blending ULSD with biodiesel resulted in suppressed (10^{-7} ohm^{-1} cm^{-2}) and elevated E_{corr} (-0.1 $V_{Hg/HgSO4}$) comparable with SS304L exposures. Visual and microscopic inspection revealed an absence of corrosion of C1020 in the presence of biodiesel (Figure 4a), even in the lowest concentration (B5). These results indicate biodiesel has a passivating effect on C1020. One possible explanation is that absorption of biodiesel to the metal surface is a barrier against water ingress. Without water in direct contact with the steel surface, corrosion is limited. However, the presence of biodiesel in L100 did not prevent active corrosion of C1020, albeit 3 orders-of magnitude

lower than exposure to neat ULSD. As illustrated in Figure 2a, the gradual decrease in E_{corr} from -0.3 $V_{Hg/HgSO4}$ (day 100) to -0.8 $V_{Hg/HgSO4}$ (day 150) also suggests a change from passive to active electrochemical behavior. Grainawi (2009) demonstrated carbon steel was most susceptible to active corrosion in ULSD without biodiesel blending. Corrosion was in the form of shallow (<5 μm) pits. These results are in agreement with the present work, which found no correlation between bulk water pH and corrosion severity.

The susceptibility of aluminum and its alloys to localized corrosion makes it particularly vulnerable to MIC. Most reports of MIC are for 99% aluminum and alloys UNS A92024 (AA2024) and UNS A97075 used in aircraft or in underground fuel storage tanks (Salvarezza et al. 1983). Two mechanisms for MIC of aluminum alloys have been documented: production of water soluble organic acids by bacteria and fungi, and formation of differential aeration cells. Several investigators reported a decrease in bulk fuel pH due to metabolites produced during growth of fungi (de Mele et al. 1979; de Meybaum and de Schiapparelli 1980; Rosales 1985). The most common isolate related to aircraft fuel and MIC is the fungus *Hormoconis resinae* (Churchill 1963; Hendey 1964; Videla et al. 1993). de Mele et al. (1979) demonstrated a correlation between growth of *Cladosporium (Homocornis)* and pH at fuel/water interfaces and measured pH values between 4.0 and 5.0. Rosales (1985) demonstrated metal ion binding by fungal mycelia, resulting in metal ion concentration cells on aluminum surfaces. de Mele et al. (1979) reported that corrosivity increased with contact time due to accumulation of metabolites under microbial colonies attached to metal surfaces. Videla (1996) demonstrated acid-etched traces of fungal mycelia on aluminum surfaces colonized by *H. resinae*. de Meybaum and de Schiapparelli (1980) demonstrated that the metabolic products enhanced aqueous phase aggressiveness even after the life cycle of *Cladosporium (Hormoconis)* was completed. In all of these reports localized corrosion attributed to MIC occurred in the water phase in the bottom of tanks and at the fuel-water interface.

Diaz-Ballote et al. (2009) reported that corrosion of aluminum (99.999% pure) exposed to biodiesel derived from canola was directly related to the concentration of residual alkaline catalysts used in the preparation. Data presented in this paper are the first report of MIC of an aluminum alloy in the fuel phase, in addition to attack at the interface and in the water layer. Pitting was observed in AA5052 for all fuel/water exposures, including biodiesel blended fuels. Great effort was taken to eliminate chloride contamination by using distilled water and a sulfate-based reference electrode. Therefore, any appreciable amount of chloride in the system was initially present in the fuel. Pits had a crystallographic appearance (Figure 8). Videla et al. (1993) observed crystallographic pits in AA2024 exposed to *H. resinae* culture in a mineral media containing <0.015 g l^{-1} chloride. Pits were formed during anodic polarization. Videla et al. (1993) likened the crystallographic pit morphology to pits formed in Cl^- solutions. For example, McNamara et al. (2005) used cross-section images to demonstrate subsurface pitting due to MIC of AA2024 in a seawater medium. Subsurface pitting in the present experiments cannot be attributed to aggressive ions, eg alkalis or chlorides, or to bulk acidic pH.

While pitting was visually observed in all AA5052 fuel/water exposures, electrochemical measurements indicated active corrosion only in L100 (Figure 6). This discrepancy is most likely due to limitations of the LPR technique. Specifically, LPR provides an instantaneous corrosion rate, ie the rate at the time of the measurement. It provides no information of corrosion that has occurred previously. Other corrosion monitoring techniques, including electrochemical noise analysis (Cottis et al. 1998; Mansfeld et al. 2001), may provide more information for electrochemical systems that alternate between active and passive behaviors.

Making electrochemical measurements in fuels is challenging because of their inherent high R_s. A Luggin probe was used in this study to minimize the ohmic potential drop (IR_s) between metal and reference electrodes. R_s was measured by EIS and used in post-measurement analysis. Addition of distilled water only moderately increased solution conductivity where R_s was orders-of-magnitude higher than R_p. To facilitate measurements and decrease R_s, charge carriers can be added in the form of salts to the fuel/water system (Farina et al. 1978; de Anna 1985; Kelly and Moran 1990; Brossia et al. 1995). However, as pointed out by Gui and Sridhar (2010) addition of a supporting electrolyte often alters the electrochemical response of the system in question. This alteration would almost certainly be observed when adding a salt to distilled water. Grainawi (2009) unsuccessfully attempted EIS measurements of carbon steel exposed in biodiesel/ULSD blended fuels with and without addition of distilled water. Videla et al. (1993) and McNamara et al. (2005) used a supporting electrolyte (minimal media) in their experiments involving AA2024 exposed in JP fuels. An alternative method to minimize IR_s effects is to decrease the amount of I flowing between the metal and reference electrodes. Decreasing the electrode size decreases the I required to polarize with a specific voltage. Gui and Sridhar (2010) successfully conducted electrochemical

measurements in fuel grade ethanol with 500 μm diameter carbon steel microelectrodes. By using microelectrodes and a Luggin probe, it may be possible to measure electrochemical properties of materials even in highly resistive media such as B100.

Another technical issue that is yet unresolved is the imaging of the fuel-covered surfaces in an ESEM. At issue is the necessity to remove coupons exposed at the fuel/water interface by passing them through the fuel layer and coating the water-exposed surface with a thin layer of fuel. If the fuel is not removed prior to placement in the ESEM, evaporating fuel condenses on the interior of the ESEM, making it impossible to image the metal surface. Removal of the fuel layer, by dissolving in organic solvents such as acetone and xylene, removes the fuel layer but also destroys a large portion of biofilm (Little et al. 1991). While removing the bulk of the fuel is trivial, removing the last surface film is more complicated.

Conclusions

Biofouling was observed in all fuel/distilled water/inoculum combinations. Microorganisms present in the original fuel samples were the dominant species characterized after a 6-month exposure. C1020 exhibited general (uniform) active corrosion in ULSD and L100, and passive behavior in B100 and biodiesel/ULSD blends. SS304L remained passive in all exposures. AA5052 was susceptible to subsurface pitting in the water and fuel layers, in addition to the fuel/water interface.

Acknowledgements

This work was supported by Dr David Shifler at the Office of Naval Research (ONR Code 332) under award N0001408WX20857. The authors would also like to acknowledge S. Williams (Naval Fuels and Lubes CFT), K. J. Johnson, R. E. Morris, and M. H. Hammond (NRL Code 6181), and B. C. Giordano (Nova Research) for the work involving fuel chemical characterization. Publication Number NRL/JA/7330-10-0331.

Abbreviations and acronyms

AA5052 – aluminum alloy UNS A95052
AA2024 – aluminum alloy UNS A92024
B5 – 5% biodiesel / 95% ultra low sulfur diesel (v/v)
B20 – 20% biodiesel / 89% ultra low sulfur diesel (v/v)
B100 – 100% biodiesel (v)
C1020 – carbon steel UNS C10200
C# – carbon atom number
DGGE – denaturing gradient gel electrophoresis
E_{corr} – corrosion potential
EIS – electrochemical impedance spectroscopy
FAME – fatty acid methyl esters
GC-MS – gas chromatography-mass spectrometry
I – current
L100 – conventional high sulfur diesel
LPR – linear polarization resistance
MIC – microbiologically influenced corrosion
ppm – parts-per-million
R_p – polarization resistance
R_p^{-1} – inverse polarization resistance
R_s – solution resistance
SS304L – stainless steel UNS S30403
ULSD – ultra low sulfur diesel
UNS – unified numbering system
V – potential

References

Agaev NM, Smorodina AE, Allakhverdova AV, Efendi-zade SM, Kosargina VG, Popov MAA. 1986. Prevention of corrosion and environmental protection. VNIIOENG (Russian) 7:1–63.

Aktas DF, Lee JS, Little BJ, Ray RI, Davidova IA, Lyles CN, Suflita JM. 2010. Anaerobic metabolism of biodiesel and its impact on metal corrosion. Energy Fuel 24:2924–2928.

Ali FA, Ghaloum N, Hauser A. 2006. Structure representation of asphaltene GPC fractions from Kuwati residual oils. Energy Fuel 20:231–238.

ASTM Standard G59-97. 2003a. Standard test method for conducting potentiodynamic polarization resistance measurements. West Conshohocken, PA: ASTM International.

ASTM Standard G1-03. 2003b. Standard practice for preparing, cleaning, and evaluating corrosion test specimens. West Conshohocken, PA: ASTM International.

ASTM Standard D5453-09. 2009. Standard test method for determination of total sulfur in light hydrocarbons, spark ignition engine fuel, diesel engine fuel, and engine oil by ultraviolet fluorescence. West Conshohocken, PA: ASTM International.

Bosecker K. 1996. Deterioration of hydrocarbons. In: Heitz E, Flemming HC, Sands W, editors. Microbiologically influenced corrosion of materials. Berlin: Springer-Verlag. p. 439–444.

Brossia CS, Gileadi E, Kelly RG. 1995. The electrochemistry of iron in methanolic solutions and its relation to corrosion. Corros Sci 37:1455–1471.

Charkraborty R, Coates JD. 2004. Anaerobic degradation of monoaromatic hydrocarbons. Appl Microbiol Biotechnol 64:437–446.

Churchill AV. 1963. Microbial fuel tank corrosion: mechanisms and contributing factors. Mater Prot 2:19–23.

Costerton JW, Boivin J. 1991. Biofilms and corrosion in biofouling and biocorrosion. In: Flemming HC, Geesey GG, editors. Industrial water systems. Berlin, Heidelberg: Springer-Verlag. p. 195–204.

Cottis RA, Al-Ansari MA, Bagley G, Pettiti A. 1998. Electrochemical noise measurements for corrosion studies. Mater Sci Forum 289–292:741–754.

Davis JR, editor. 1998. Metals handbook. 2nd ed. Materials Park, OH: ASM International.

de Anna PL. 1985. The effects of water and chloride ions on the electrochemical behaviour of iorn and 304L stainless steel in alcohols. Corros Sci 25:43–53.

de Mele MFL, Salvarezza RC, Videla HA. 1979. Microbial contaminants influencing the electrochemical behavior of aluminum and its alloys in fuel-water systems. Int Biodeterior Bull 15:39–44.

de Meybaum BR, de Schiapparelli ER. 1980. A corrosion test for determining the quality of maintenance in jet fuel-storage. Mater Perf 19:41–44.

Diaz-Ballote L, Lopez-Sansores JF, Maldonado-Lopez L, Garfias-Mesias LF. 2009. Corrosion behavior of aluminum exposed to a biodiesel. Electrochem Comm 11:41–44.

Farina CA, Faita G, Olivani F. 1978. Electrochemical behavior of iron in methanol and dimethylformamide solutions. Corros Sci 18:465–479.

Fischer SG, Lerman LS. 1979. Length-independent separation of DNA restriction fragments in two-dimensional gel electrophoresis. Cell 16:191–200.

Gieg LM, Duncan KE, Suflita JM. 2008. Bioenergy production *via* microbial conversion of residual oil to natural gas. Appl Environ Microbiol 74:3022–3029.

Grainawi L. 2009. Testing for compatibilty of steel with biodiesel. Paper presented at CORROSION/2009; March 22–26; Atlanta, GA. Houston, TX: NACE International. p. 1–19.

Gui F, Sridhar N. 2010. Condueting eleetroehemieal measurements in fuel-grade ethanol using microelectrodes. Corrosion 66:045005-1-8.

Heider J. 2007. Adding handles to unhandy substrates: anaerohic hydrocarbon activation mechanisms. Curr Opin Chem Biol 11:188–194.

Hendey NI. 1964. Some observations on *Cladosporium resinae* as a fuel contaminant and its possible role in corrosion of aluminium alloy fuel tanks. Br Mycol Soc Trans 47:467–475.

Jackson CR, Roden EE, Churchill PF. 2000. Denaturing gradient gel electrophoresis can fail to separate 16S rDNA fragments with multiple base differences. Mol Biol Today 1:49–51.

Johnson KJ, Rose-Pehrsson SL, Morris RE. 2004. Monitoring diesel fuel degradation by gas chromatography-mass spectroscopy and chemometric analysis. Energy Fuel 18:844–850.

Kaul S, Saxena RC, Kumar A, Negi MS, Bhatnagar AK, Goyal HB, Gupta AK. 2007. Corrosion behavior of biodiesel from seed oils of Indian origin on diesel engine parts. Fuel Process Technol 88:303–307.

Kelly RG, Moran PJ. 1990. The passivity of metals in organic solutions. Corros Sci 30:495–509.

Knothe G, Steidley KR. 2005. Luhricity of components of biodiesel and petrodiesel. The origin of biodiesel lubricity. Energy Fuel 19:1192–1200.

Little BJ, Wagner PA, Ray RI, Pope RK, Scheetz R. 1991. Biofilms: an ESEM evaluation of artifacts introduced during SEM preparation. J Ind Microbiol 8:213–222.

Lockridge D. 2007. New fuels, new problems. Heavy Duty Trucking 86:30–48.

Londry KL, Suflita JM. 1998. Toxicity effects of organosulfur compounds on anaerobic microbial metabolism. Environ Toxicol Chem 17:1199–1206.

Lutz G, Chavarria M, Arias ML, Mata-Segreda JF. 2006. Microbial degradation of palm (*Elaeis guineensis*) biodiesel. Rev Biol Trop 54:59–63.

Mansfeld F, Sun Z, Hsu CH. 2001. Electrochemical noise analysis (ENA) for aetive and passive systems in chloride media. Electrochim Acta 46:3651–3664.

McNamara CJ, Perry TD, Wolf N, Mitchell R, Leard R, Dante J. 2003. Corrosion of aluminum 2024 by jet fuel degrading microorganisms. Paper presented at CORROSION/2003; San Diego, CA. Houston, TX: NACE International. p. 1–6.

McNamara CJ, Perry TD, Leard R, Bearce K, Dante J, Mitchell R. 2005. Corrosion of aluminum alloy 2024 by microorganisms isolated from aircraft fuel tanks. Biofouling 21:257–265.

Meckenstock RU, Safinowski M, Griebler C. 2004. Anaerobic degradation of polycyclic aromatic hydrocarhons. FEMS Microbiol Ecol 49:27–36.

Mecnakshi HN, Shyamala R, Saratha R, Papavinsaam S. 2010. Corrosion of metals in biodiesel from *Pongamia pinnata*. Paper presented at CORROSION/2010; March 14–18; San Antonio, TX. Houston, TX: NACE International. p. 1–16.

Melero JA, Calleja G, Garcia A, Clavero M, Hernandez EA, Miravalles R, Galindo T. 2010. Storage stahility and corrosion studies of renewable raw materials and petrol mixtures: a key issue for their co-processing in refinery units. Fuel 89:554–562.

Muyzer G, Smalla K. 1998. Application of denaturing gradient gel electrophoresis (DGGE) and temperature gradient gel electrophoresis (TGGE) in microhial ecology. Antonie Leeuwenhoek 73:127–141.

Rabus R. 2005. Biodegradation of hydrocarbons under anoxic conditions. In: Ollivier B, Magot M, editors. Petroleum microbiology. Washington: ASM Press. p. 277–299.

Ray R, Little B. 2003. Environmental electron microscopy applied to hiofilms. In: Lens P, Moran AP, Mahony T, Stoodley P, O'FLaherty V, editors. Biofilms in medicine, industry and environmental hiotechnology. London, UK: IWA Publishing. p. 331–351.

Rosales BM. 1985. Corrosion measurements for determining the quality of maintenance in jet fuel storage. Paper presented at Argentine – USA Workshop on Biodeterioration; La Plata, Argentina, Sao Paulo, Brazil: Aquatec Quimica SA. p. 135–143.

Salvarezza RC, de Mele MFL, Videla HA. 1983. Meehanisms of the microhial corrosion of aluminum alloys. Corrosion 39:26–32.

Siddique T, Fedorak PM, MacKinnon MD, Foght JM. 2007. Metabolism of BTEX and naphtha compounds to methane in oil sands tailings. Environ Sci Technol 41:2350–2356.

Suflita JM, McInerney MJ. 2008. Microbial approaches for the enhanced recovery of methane and oil from mature reservoirs. In: Wall JD, Harwood CS, Demain A, editors. Bioenergy. Washington: ASM Press. p. 389–403.

Suflita JM, Davidova IA, Gieg LM, Nanny M, Prince RC. 2004. Anaerobic hydrocarhon hiodegradation and the prospects for microbial enhanced energy production. In: Vazquez-Duhalt R, Quintero-Ramierez R, editors. Petroleum biotechnology: developments and perspectives. New York: Elsevier BV. p. 283–305.

Townsend GT, Prince RC, Suflita JM. 2004. Anaerohie biodegradation of alicyclic constituents of gasoline and natural gas condensate by bacteria from an anoxic aquifer. FEMS Microbiol Ecol 49:129–135.

Videla HA. 1996. Manual of hiocorrosion. Boca Raton: CRC Press.

Videla HA, Guiamet PS, DoValle S, Reinoso EH. 1993. Effects of fungal and bacterial contaminants of kerosene fuels on the corrosion of storage and distribution systems. In: Kobrin G, editor. A practical manual on microbiologically influenced corrosion. Houston, TX: NACE International. p. 125–139.

Wang J, Ma T, Zhao LX, Lv JH, Li GQ, Zhang H, Zhao B, Liang FL, Liu RL. 2008. Monitoring exogenous and indigenous bacteria by PCR-DGGE technology during the process of microbial enhanced oil recovery. J Ind Microbiol Biotechnol 35:619–628.

Watkinson RJ. 1984. Hydrocarbon degradation. Microbial problems and corrosion in oil and oil products storage. London: The Institute of Petroleum. p. 50–56.

Widdel F, Rabus R. 2001. Anaerobic biodegradation of saturated and aromatic hydrocarbons. Curr Opin Biotechnol 12:259–276.

Zhang X, Peterson C, Reece D, Haws R, Moller G. 1998. Biodegradability of biodiesel in the aquatic environment. Trans ASAE 41:1423–1430.